

Design philosophy and method for modern high-current, radio-frequency quadrupole accelerators with low emittance transfer

Chuan Zhang ^{1, #}, Holger Podlech ²

¹ *GSI Helmholtz Center for Heavy Ion Research, Planckstr. 1, Darmstadt, Germany*

² *Institute for Applied Physics, Goethe-University, Frankfurt a. M., Germany*

Abstract

Modern radio frequency quadrupole (RFQ) accelerators are facing the challenges of space charge effects due to increased demands on beam current. This study investigated how to reach good beam quality and a compact structure simultaneously by avoiding emittance transfer. A design philosophy which holds the ratio of the longitudinal and transverse emittances at 1.0 as well as requires the ratio of the longitudinal and transverse phase advances to be in the range of 0.5 ~ 2.0 is being proposed. The application of this design philosophy integrated with the so-called BABBLE/NFSP method for a high current, high frequency, high injection energy RFQ accelerator is described.

Keywords: Radio frequency quadrupole accelerator; Beam dynamics; High current; Space charge effects; Emittance transfer

PACS: 28.65.+a; 29.20.Ej; 29.25.Dz; 29.27.Bd

[#] e-mail: c.zhang@gsi.de

I. INTRODUCTION

The R & D of a new generation of high power proton accelerators (HPPA) with beam energies up to several GeV and power levels up to several MW has become a common interest for the particle accelerator community. Modern HPPA machines are of significant importance for promoting not only basic research but also advanced civil applications, because they can serve as spallation neutron sources, radioactive beam facilities, factories for other interesting secondary particles e.g. antiprotons and neutrinos, or accelerator-driven systems.

There are mainly three factors to increase the beam power i.e. beam energy, beam duty factor, and beam current. Increasing the beam energy and the beam duty factor will bring most challenges to the accelerator technology development, while increasing the beam current can make the beam dynamics design more demanding, especially for the radio frequency quadrupole (RFQ) accelerator. This is because the lower the beam energy is, the stronger the space-charge effects are. As the standard injector to modern HPPA machines, the RFQ accelerator could be a bottleneck to the performance of the whole facility.

A worldwide survey of achieved and planned hadron accelerator power frontiers including HPPA projects can be found in an overview plot from [1]. Some HPPA facilities accelerate protons directly, while some accelerate negative hydrogen ions in the linac part first and then strip two electrons from each ion at the injection into the synchrotron, which has the advantages to reduce the space charge effects at the synchrotron injection, accumulate more particles in the synchrotron, and lead to a higher beam brilliance consequently. The difference in accelerating H^+ versus H^- particles plays almost no role for the beam dynamics in the accelerator.

TABLE I lists the main design parameters of some running high current H^+ or H^- RFQ accelerators [2-6] realized for the HPPA projects, SNS, J-PARC, CSNS, and KOMAC, which appeared in the above-mentioned overview plot. Besides, two other similar machines, the LINAC4 RFQ [7] and the CPHS RFQ [8] are also included for a more comprehensive list. It can be seen that the typical frequency and output beam energy for the listed RFQ accelerators are 325 ~ 350MHz and 3MeV, respectively, except those parameters of the earlier SNS RFQ are a little different.

The purpose of this study is trying to find a helpful design philosophy towards efficient RFQ accelerators of this type with both good beam quality and a compact structure. Therefore, a representative RFQ has been conceived and adopted, based on the following careful considerations on the choices of its basic parameters:

- f (frequency) = 325MHz: the lowest value of the listed RFQs for challenging the compactness as well as for having a higher current limit [9].
- W_{out} (output beam energy) = 3MeV: the typical value of the listed RFQs.
- I_{in} (design beam current) = 70mA: the highest value of the listed RFQs. A further requirement imposed on this study is that this RFQ should be able to work at higher currents up to 100mA in order to challenge more serious space charge effects.
- W_{in} (input beam energy) = 95keV and $\epsilon_{\text{in, trans., n., rms}}$ (normalized rms transverse input emittance) = $0.3 \pi \text{ mm mrad}$: as mentioned, the studied RFQ is supposed to be also feasible for a 100mA input beam, so relatively higher input energy to relax the space charge effects and relatively larger input emittance according to the state of the art ion source technology have been taken.
- U (inter-vane voltage): 80kV, moderate among the listed RFQs.

For a convenient description, this high current, high frequency, high injection energy RFQ is called as the HHH RFQ in the following text. The design goals of this RFQ are as the follows:

- The total structure length should be kept at $\sim 3\text{m}$, which is quite demanding, because its input energy is almost double that of the other listed RFQs, but it is well known that the length of the adiabatic bunching section is proportional to β^3 [10].
- The beam transmission should be $\geq 95\%$ and $\geq 90\%$ for the design current 70mA and the required higher current 100mA, respectively.
- Besides, good beam quality especially small emittance growth is required to meet the demands for modern accelerators e.g. no quenching of downstream SC cavities, hands-on maintenance, high reliability, and so on.

TABLE I. Design parameters of some realized 325 ~ 350MHz, 3MeV RFQs and design requirements for the HHH RFQ.

	SNS	J-PARC RFQ-III	CSNS	KOMAC (PEFP)	CPHS	CERN LINAC 4	HHH
Ion	H ⁻	H ⁻	H ⁻	H ⁺	H ⁺	H ⁻	H ⁺
f [MHz]	402.5	324	324	350	325	352.2	325
W_{in} [keV]	65	50	50	50	50	45	95
W_{out} [MeV]	2.5	3.0	3.0	3.0	3.0	3.0	3.0
I_{in} [mA]	60	60	40	20	50	70	70 ~ 100
U [kV]	83	81	80	85	60-135	78	80
$\mathcal{E}_{\text{in, trans., n., rms}}$ [π mm mrad]	0.20	0.20	0.20	0.20	0.20	0.25	0.30
L [m]	3.7	3.6	3.6	3.2	3.0	3.0	~3.0
T [%]	>90	98.5	97.1	98.3	97.2	95	≥ 95 for 70mA ≥ 90 for 100mA

II. DESIGN PHILOSOPHY FOR LOW EMITTANCE TRANSFER

To reach high beam transmission as well as keep good beam quality for a high current RFQ accelerator, one crucial issue is how to avoid beam instabilities induced by emittance transfer during the beam bunching and acceleration process. For intense beams, the coupling-related resonances play a remarkable role in causing beam instabilities. An ideal linac beam should be isotropic i.e. the charge density distribution everywhere inside the beam is the same and the energy between different degrees of freedom is balanced. In reality, the beam is usually anisotropic, and instinctive charge redistribution and energy transfer will take place in order to return to the equilibrium state, unfortunately at the cost of emittance growth.

Systematic studies on collective instabilities for anisotropic beams have been done by I. Hofmann since several decades [11]. By imposing perturbations on an anisotropic Kapchinsky-Vladimirsky distribution in a constant focusing system with arbitrary focusing ratios and emittance ratios,

calculations of the Vlasov equation in two transverse dimensions were performed. Though no 3D self-consistent analysis has been found so far, I. Hofmann suggested that the same mechanisms of instability and similar thresholds could be applied for the longitudinal-transverse coupling resonances as well [12]. For different emittance ratios, the growth rates and thresholds of the coupling-related resonances can be identified and visualized in the so-called “Hofmann Instability Charts” by two dimensionless parameters namely the tune ratio σ_l/σ_t and the tune depression σ/σ_0 , where $\frac{\sigma}{\sigma_0} = 1$ represents the zero-current case and $\frac{\sigma}{\sigma_0} \leq 0.4$ for space-charge-dominated cases, respectively.

On the charts, the shaded areas indicate the positions for emittance transfer and the developing speed of these parametric resonances. Usually, the “peaks” of the coupling-related resonance appear when $\frac{\sigma_l}{\sigma_t} = \frac{m}{n}$ (m and n are integers), e.g. at the positions: 0.5, 1.0, 1.5, 2.0, etc. Actually, such coupling resonances also exist at zero current because of the RF defocusing effect coming with the negative synchronous phase, however, the stop bands are significantly widened in the presence of strong space charge effects.

On the Hofmann Charts, the maximum spread of the safe tune depression (namely not shaded) always appears at the location of the dashed line, where $\frac{\sigma_t}{\sigma_l} = \frac{\varepsilon_l}{\varepsilon_t}$ is satisfied and a resonance peak expected to be present is “killed”. Because this condition can reach an energy-balanced beam and provide no free energy for driving the resonances, it is known as the equipartitioning condition [13]. Taking this as a useful guideline, a so-called “Equipartitioning Procedure” (EP) was developed and applied for the beam dynamics design of a 140mA deuteron RFQ [14]. The simulation results have proven that the EP design is successful and it is robust against very strong space charge effects.

Many studies e.g. [15, 16, 3] have shown that good beam quality as well as a compact structure can be also achieved without a strict EP design but by putting the beam trajectories in the clear area on the Hofmann Charts or letting them cross the resonance peaks quickly. However, there is no clear recipe to control the beam trajectories. This study is aiming to find useful hints from the Hofmann Charts and propose operable design guidelines for avoiding emittance transfer.

For an RFQ, the input beam from the ion source is typically a DC beam with very small energy spread, so in an RFQ beam dynamics design study the input longitudinal emittance ε_l is usually taken as 0. Along with the bunching process, ε_l will be gradually increased to the final value. This study is focusing on the Hofmann Charts in this range of the emittance ratio $\frac{\varepsilon_l}{\varepsilon_t}$ between 0.1 to 2.0. For a clearer observation, the charts have been divided into two groups and overlapped with each other in FIG. 1 for $\frac{\varepsilon_l}{\varepsilon_t} = 0.1$ to 1.0 (from the back to the front) and FIG. 2 for $\frac{\varepsilon_l}{\varepsilon_t} = 1.0$ to 2.0 (from the front to

the back), respectively, where the dashed lines are marking the EP positions. The charts were generated using the TraceWin Code [17]. For both figures, the interval of the emittance ratios is 0.1.

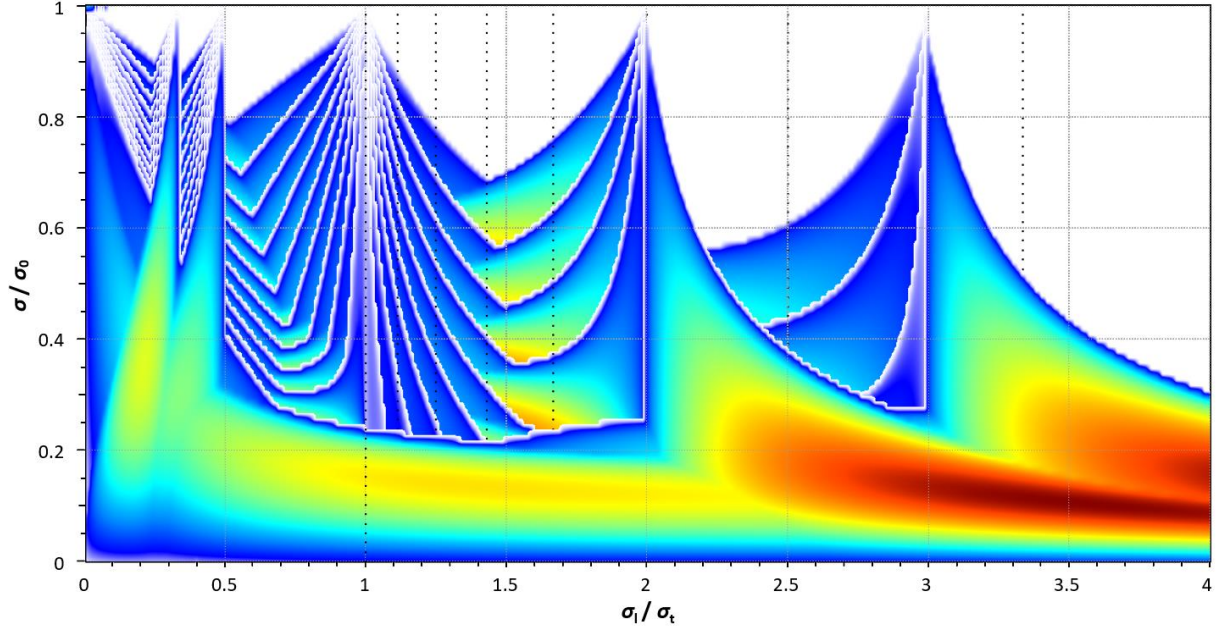


FIG. 1. Overlapped Hofmann Charts for emittance ratios $\frac{\varepsilon_l}{\varepsilon_t} = 0.1$ to 1.0 (from the back to the front).

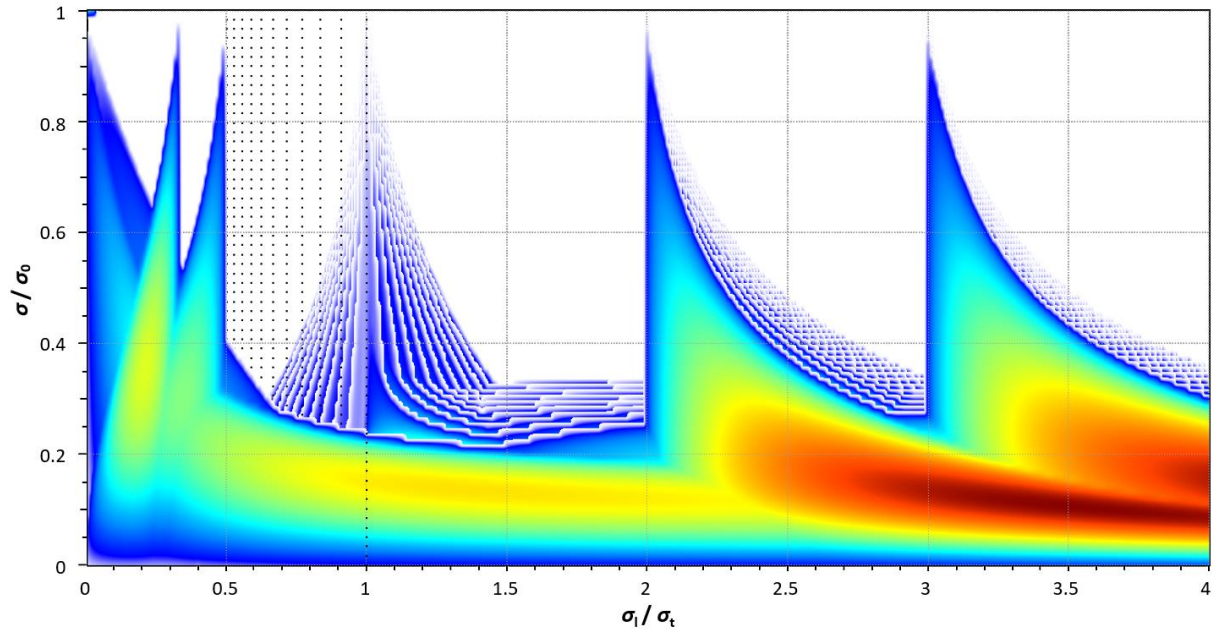


FIG. 2. Overlapped Hofmann Charts for emittance ratios $\frac{\varepsilon_l}{\varepsilon_t} = 1.0$ to 2.0 (from the front to the back).

Both FIG. 1 and FIG. 2 indicate that the largest safe place for the beam trajectories is the quasi-rectangle area which ranges from 0.5 to 2.0 in the $\frac{\sigma_l}{\sigma_t}$ direction and from ~ 0.2 to 1.0 in the $\frac{\sigma}{\sigma_0}$ direction, respectively, on the $\frac{\varepsilon_l}{\varepsilon_t} = 1.0$ Hofmann Chart. A clear signal here is that if the two conditions, namely $\frac{\varepsilon_l}{\varepsilon_t} = 1.0$ and $\frac{\sigma_l}{\sigma_t} = 0.5$ to 2.0, can be satisfied simultaneously, the biggest tolerance for changing beam

parameters will be available and emittance transfer can be maximally avoided. In short, it is called as the $\frac{\varepsilon_l}{\varepsilon_t}=1.0$ design philosophy.

III. DESIGN & SIMULATION RESULTS OF THE HHH RFQ

The concrete beam dynamics design of the 70mA HHH RFQ has been achieved using the so-called “Balanced and Accelerated Beam Bunching at Low Energy” (BABBLE) method which was previously known as “New Four-Section Procedure” (NFSP) [15, 18] in combination with the $\frac{\varepsilon_l}{\varepsilon_t}=1.0$ design philosophy. Different from the traditional “LANL Four-Section Procedure” [19], the BABBLE/NFSP method divides the whole RFQ into three sections: a main bunching (MB) section, a mixed-bunching-acceleration (MBA) section, and a main acceleration (MA) section. Along the bunching process, meanwhile, the transverse focusing strength B is varying instead of being kept constant due to the changing space-charge situation [15, 18]. The BABBLE/NFSP method has enabled several efficient RFQ designs e.g. [15, 20] with both compact length and good beam performance, even at very high beam intensities e.g. 200 mA [18].

The $\frac{\varepsilon_l}{\varepsilon_t}=1.0$ design philosophy was implemented into the BABBLE/NFSP design in the following way. During the MB stage, usually the longitudinal emittance of the beam will be gradually increased from ~ 0 to a certain value. If the RFQ is well designed, the longitudinal emittance at the end of the MB section can be maintained in the rest part of the RFQ until the exit. Therefore, in some sense, the MB section can be called as the “longitudinal emittance formation phase” and its final ε_l value can be regarded as the “real” longitudinal input emittance. To apply the $\frac{\varepsilon_l}{\varepsilon_t}=1.0$ design philosophy, our idea is to let the BABBLE/NFSP design of the HHH RFQ stop the MB section when the “real” longitudinal input emittance almost equals to the transverse emittance and then continue the MBA and MA sections.

In order to take advantage of the largest safe place on the Hofmann Charts, it is not sufficient to keep $\frac{\varepsilon_l}{\varepsilon_t}=1.0$ only. At the same time, the $\frac{\sigma_l}{\sigma_t}$ value of the beam should be limited within the range of 0.5~2.0. The phase advance σ_l and σ_t represent the longitudinal and transverse focusing strength, respectively. The LANL method holds B constant for the main RFQ, so usually σ_t is already very big at the end of the radial matching section where σ_l is still close to zero, which is not favourable to

quickly increase $\frac{\sigma_l}{\sigma_t}$ to a value ≥ 0.5 . On the other side, when the main acceleration starts, the space charge effects will be weakened naturally, so it is also not reasonable to keep B as strong as before.

The strategy of the BABBLE/NFSP method is to adjust the B value according to the space-charge situation along the RFQ: 1) B starts with a relatively small value; 2) then it will be increased in the MB and MBA sections to balance the increased longitudinal focusing; 3) and afterwards when the MA section starts, B falls down accordingly. In this way, the σ_t and σ_l can have relatively similar evolution tendencies in most part of the RFQ, which will help the beam to satisfy the condition $\frac{\sigma_l}{\sigma_t} = 0.5 \sim 2.0$. In this way, a $\frac{\varepsilon_l}{\varepsilon_t} = 1.0$ beam can have minimum emittance transfer between longitudinal and transverse planes.

The evolutions of the three main beam dynamics parameters i.e. electrode aperture, electrode modulation and synchronous phase along the designed HHH RFQ are shown in FIG. 3. The beam dynamics simulation was performed using the PARMTEQM code [21] with a 4D-Waterbag input distribution.

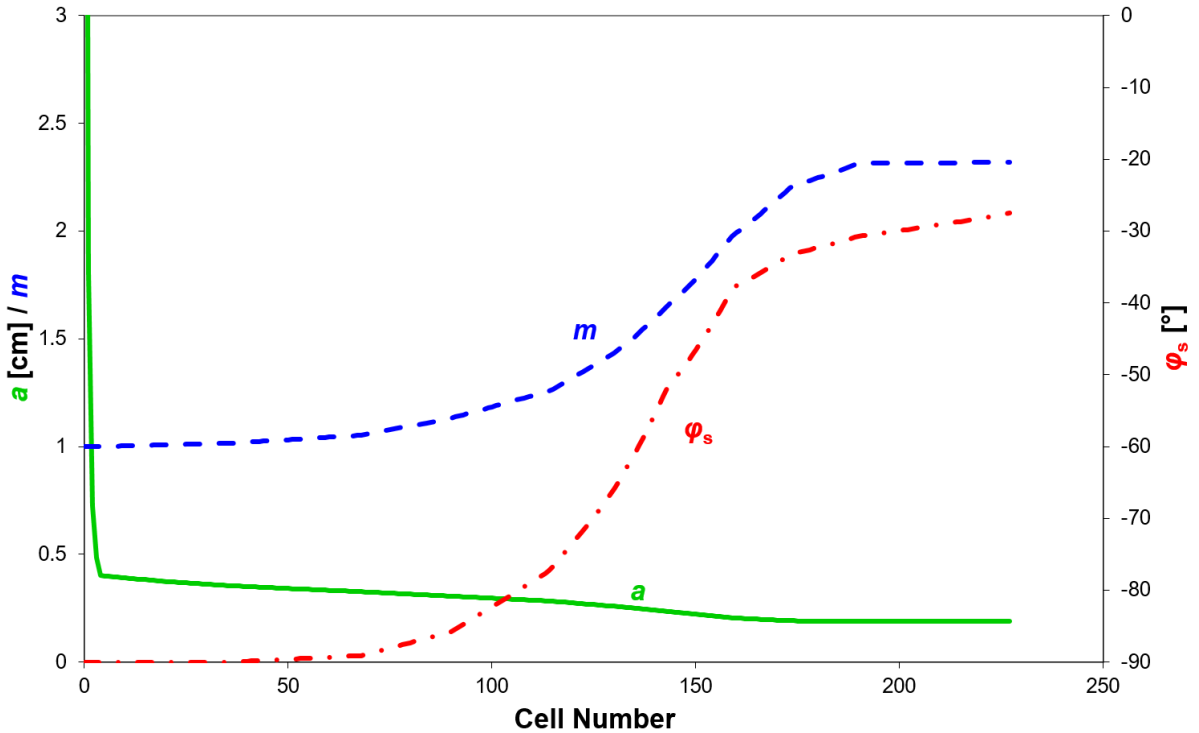


FIG. 3. Main beam dynamics design parameters of the RFQ.

FIG. 4 plots several key ratios of the beam parameters for our analyses, where b and a are the longitudinal and transverse rms beam sizes in mm, respectively. The BABBLE/NFSP partitions of the HHH RFQ can also be distinguished in the figure: 1) MB: Cell 0 to Cell 90; 2) MBA: Cell 71 to Cell 150, which is also a quasi-EP section; 3) MA: Cell 151 to the exit. At the end of the MB section,

$\frac{\varepsilon_l}{\varepsilon_t}$ reaches ~ 1.0 and the beam starts to enter the range of $\frac{\sigma_l}{\sigma_t} = 0.5$ to 2. Afterwards, the emittance ratio is kept at ~ 1.0 , although $\frac{\sigma_l}{\sigma_t}$ drops to the ≤ 0.5 region again in the last cells.

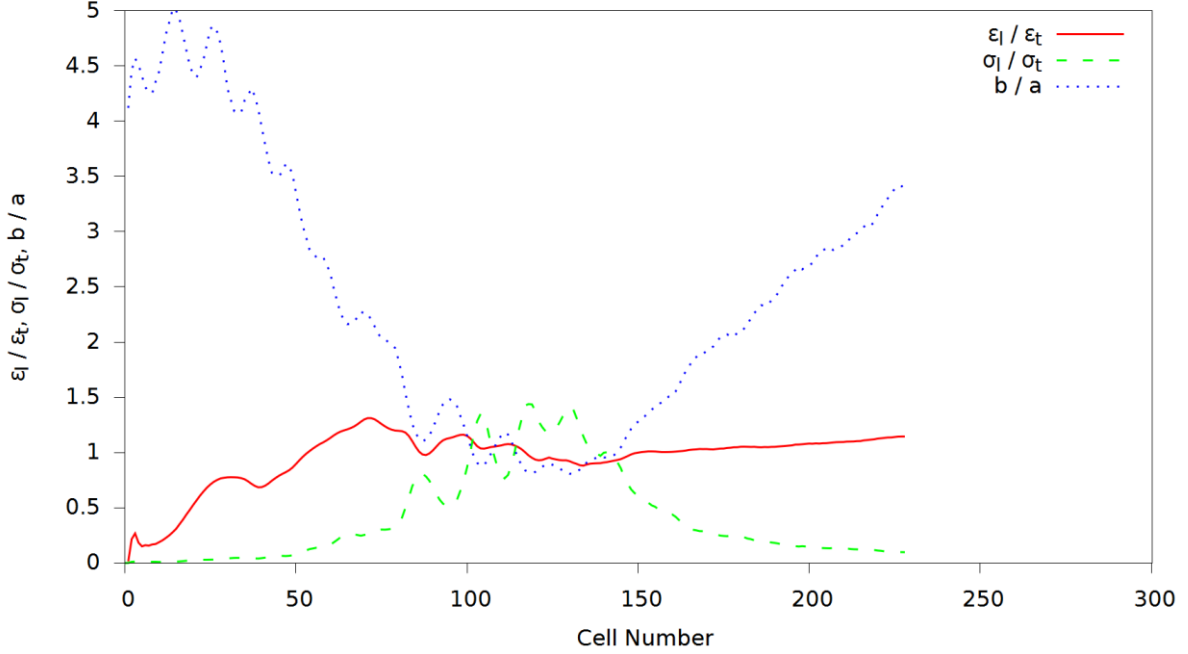


FIG. 4. Ratios of emittances, phase advances, and beam sizes along the RFQ.

The beam footprints of the HHH RFQ on the $\frac{\varepsilon_l}{\varepsilon_t} = 1.0$ Hofmann Chart are shown in FIG. 5. The different sections are marked in different colors i.e. red for MB, green for MBA, and blue for MA, respectively. Meanwhile, the solid and dashed curves stand for the tune depressions in the transverse and longitudinal directions, respectively. It can be seen that the beam trajectories are mainly locating in the safe places on the chart so that this kind of bunching process can be performed much faster than that in the LANL-style gentle buncher section. This will consequently lead to a compact structure. In the main acceleration section, the beam trajectories especially in the longitudinal plane step into the instability region, but it is not so harmful, because the period is short and the space charge effects are already weakened by the quickly increased beam velocity.

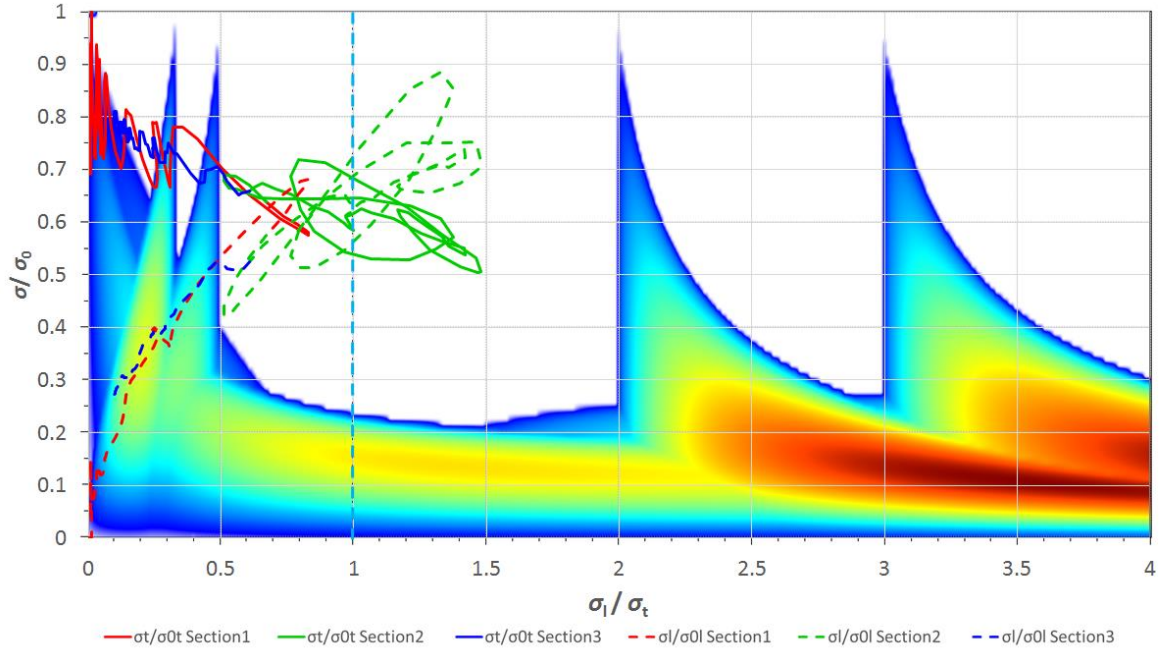


FIG. 5. Beam footprints of the RFQ at 70mA on the $\frac{\varepsilon_l}{\varepsilon_t} = 1.0$ Hofmann Chart.

As required, the HHH RFQ should be also able to work for higher currents up to 100mA. FIG. 6 checks the beam footprints of the HHH RFQ at 100mA. Generally speaking, the behavior of the beam is still similar to that in the 70mA case. Of course, from 70mA to 100mA, the space charge effects are getting stronger, so the “gravity center” of the beam trajectories has been lowered from ~ 0.65 to ~ 0.55 in the $\frac{\sigma}{\sigma_0}$ direction. But there is still sufficient clean place below the beam trajectories, which gives a hint that this RFQ can work for even higher currents.

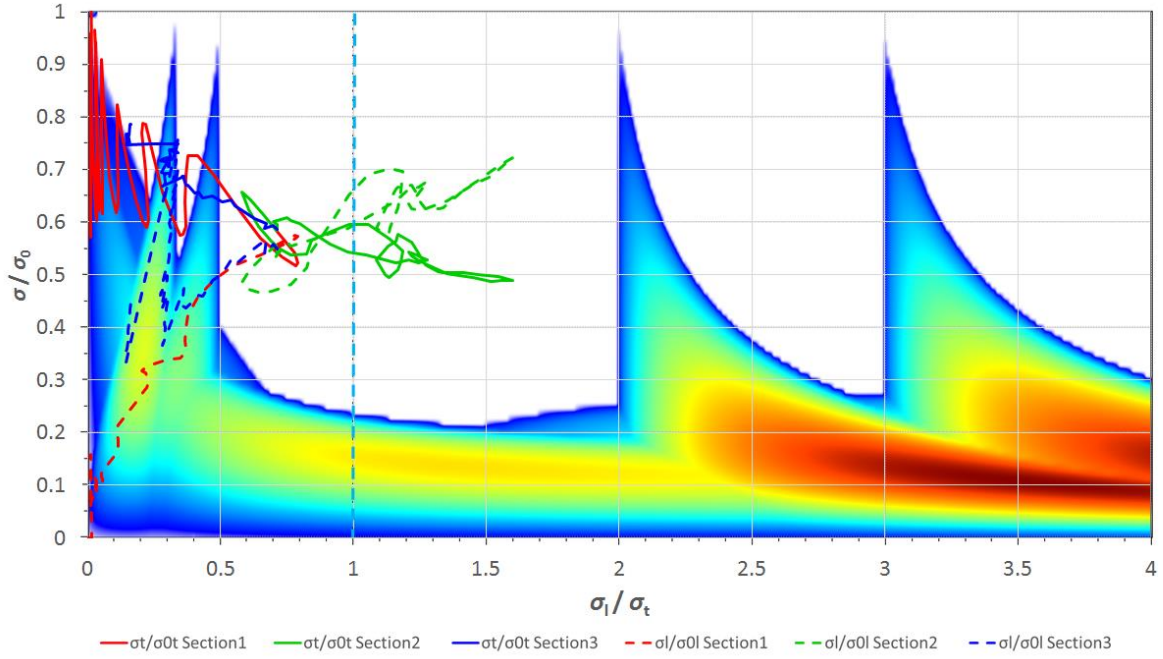


FIG. 6. Beam footprints of the RFQ at 100mA on the $\frac{\varepsilon_l}{\varepsilon_t} = 1.0$ Hofmann Chart.

Furthermore, the ratios of the longitudinal and transverse emittances as well as phase advances along the RFQ for both 70mA and 100mA are compared in FIG. 7. The evolutions of these parameters are fairly close to each other, except the emittance ratio of the 100mA beam has a few “jumps” in the main acceleration section. From the curve of the emittance ratio calculated with the longitudinal emittance for 99% instead of 100% of the beam, it can be known that this difference has been caused by only $\leq 1\%$ of halo particles.

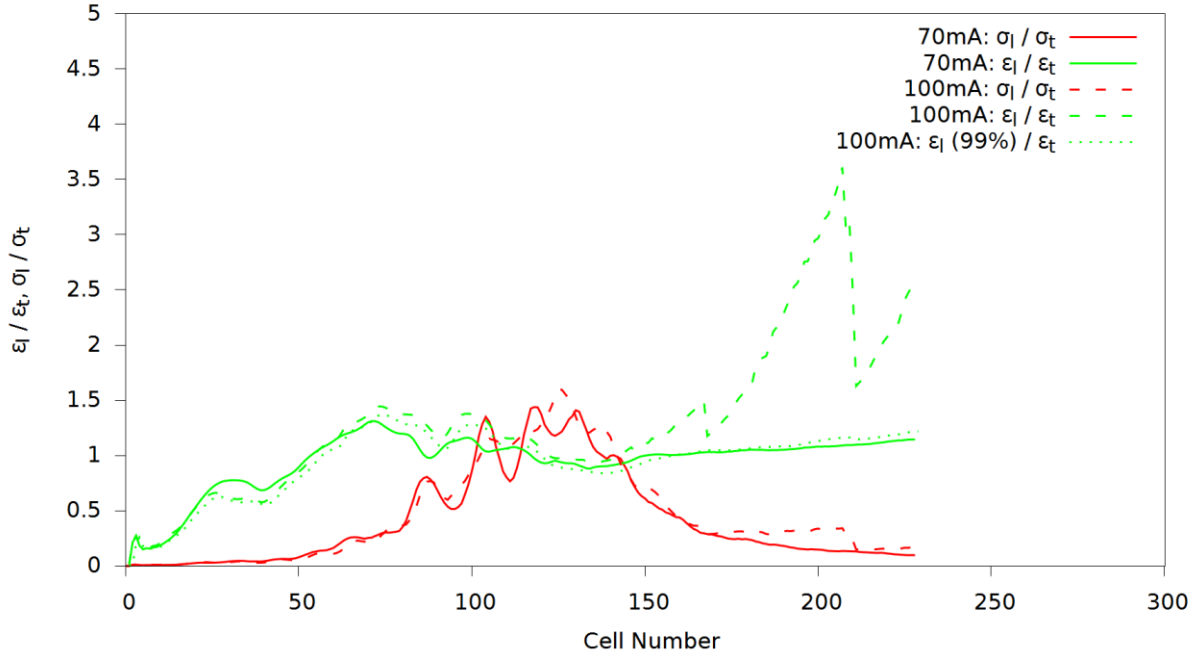


FIG. 7. Comparison of emittance ratios and phase advance ratios between 70mA and 100mA.

FIG. 8 shows the output particle distributions not only in the three phase spaces but also with the front, side and top views in the real space. Again, it shows the similarity between 70mA and 100mA, except the 100mA beam has slightly bigger beam sizes especially in the longitudinal direction. But in both cases, the beam is still well concentrated.

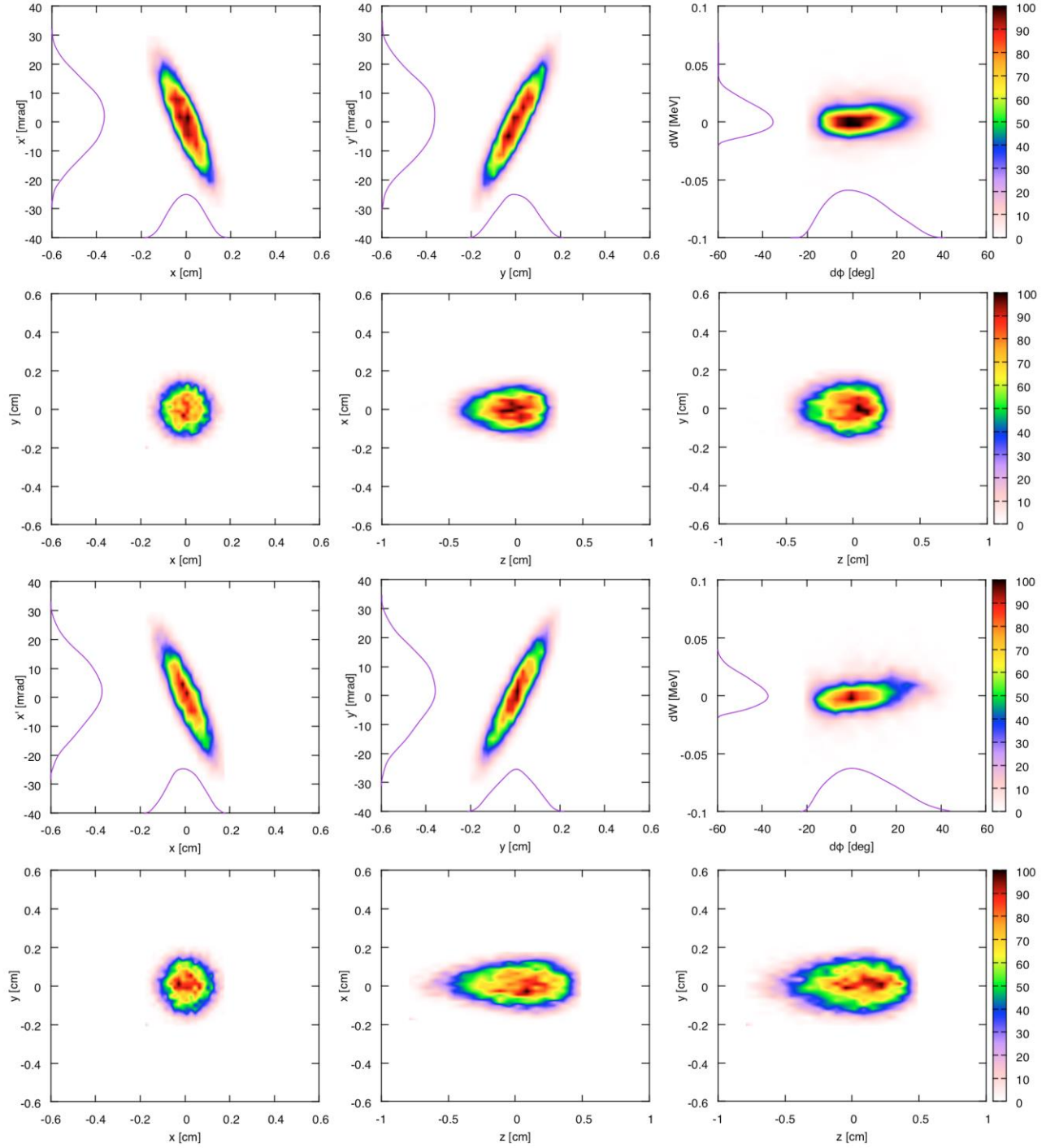


FIG. 8. Output particle distributions (top: 70mA; bottom: 100mA).

More detailed design and simulation results of the HHH RFQ at both 70mA and 100mA are given in TABLE II. The design goals with respect to transmission efficiency have been well fulfilled. Even the design is not optimized for 100mA and there are some mismatching issues, the transmission is still close to 91%. Also, the 3.15m-long HHH RFQ is relatively compact, especially

when we take into account its considerably high injection energy. The transverse emittance growths for both cases are almost ignorable, only 1 ~ 2%. Compared with some other RFQs in the table, the HHH RFQ has slightly larger but not very different longitudinal output emittance. This is because the given transverse input emittance of the HHH RFQ is already 50% or 20% bigger than that of the other machines and the HHH RFQ design follows the $\frac{\varepsilon_l}{\varepsilon_t} = 1.0$ design philosophy.

TABLE II. Main design results of some realized 325 ~ 350MHz, 3MeV RFQs and the HHH RFQ.

	SNS	J- PARC RFQ- III	CSNS	KOMAC (PEFP)	CPHS	CERN LINAC4	HHH 70mA	HHH 100mA
U [kV]	83	81	80	85	60- 135	78	80	80
I_{in} [mA]	60	60	40	20	50	70	70	100
f [MHz]	402.5	324	324	350	325	352.2	325	325
W_{in} [keV]	65	50	50	50	50	45	95	95
W_{out} [MeV]	2.5	3.0	3.0	3.0	3.0	3.0	3.0	3.0
$\mathcal{E}_{\text{in, trans., n., rms}}$ [π mm mrad]	0.20	0.20	0.20	0.20	0.20	0.25	0.30	0.30
$\mathcal{E}_{\text{out, x, n., rms}}$ [π mm mrad]	0.21	0.21	0.2002	0.22	0.246	0.25	0.304	0.304
$\mathcal{E}_{\text{out, y, n., rms}}$ [π mm mrad]	0.21	0.21	0.2002	0.22	0.248	0.25	0.305	0.306
$\mathcal{E}_{\text{out, z, rms}}$ [keV-deg]	103	110	114.3	112	144	130	128 (118 for 99% of the beam)	283 (136 for 99% of the beam)
L [m]	3.7	3.6	3.62	3.24	3.0	3.0	3.15	3.15
T [%]	>90	98.5	97.1	98.3	97.2	95	96.5	90.7

IV. CONCLUSIONS

In order to avoid the beam instabilities caused by emittance transfer for modern high current RFQ accelerators, a so-called $\frac{\varepsilon_l}{\varepsilon_t} = 1.0$ design philosophy has been proposed. Combined with the practical BABBLE/NFSP design method, it can be very helpful to take advantage of the largest safe area on the Hofmann Charts for the beam motions.

With typical basic parameters for modern high current RFQ accelerators, a representative RFQ has been conceived and chosen for the investigation. The achieved good performance at both 70mA and 100mA has demonstrated the feasibility of the combination of the $\frac{\varepsilon_l}{\varepsilon_t} = 1.0$ design philosophy and the BABBLE/NFSP method to lead to good beam quality and compact length simultaneously.

The $\frac{\varepsilon_l}{\varepsilon_t} = 1.0$ design philosophy is not necessary a must-have condition but a useful guideline towards efficient high current RFQs for modern applications. As the Hofmann Charts are general for accelerator beams, it can be also applied to high current drift tube linac designs.

ACKNOWLEDGEMENTS

The author CZ would like to thank Eugene Tanke very much for his friendly and patient help which enabled a deep look inside the design and convenient data analyses as well as his valuable suggestions for the improvement of the manuscript.

REFERENCES

- [1] J. Wei *et al.*, in *Proceedings of LINAC2016* (JACoW, East Lansing, USA, 2016), p. 1.
- [2] A. Ratti *et al.*, in *Proceedings of LINAC1998* (JACoW, Chicago, USA, 1998), p. 276.
- [3] Y. Kondo, K. Hasegawa, T. Morishita, and R.A. Jameson, Beam dynamics design of a new radio frequency quadrupole for beam-current upgrade of the Japan Proton Accelerator Research Complex linac, *Phys. Rev. ST Accel. Beams* **15**, 080101 (2012).
- [4] S. Fu *et al.*, in *Proceedings of LINAC2006* (JACoW, Knoxville, USA, 2006), p. 222.
- [5] Y.-S. Cho *et al.*, in *Proceedings of IPAC2013* (JACoW, Shanghai, China, 2013), p. 2052.
- [6] Y. S. Cho, H. J. Kwon, J. H. Jang, H. S. Kim, K. T. Seol, D. I. Kim, Y. G. Song, and I. S. Hong, The PEPF 20-MeV Proton Linear Accelerator, *J. of Korea Phys. Soc.* **52**, 721 (2008).
- [7] C. Rossi *et al.*, in *Proceedings of LINAC2008* (JACoW, Victoria, Canada, 2008), p. 157.
- [8] Q.Z. Xing, Y.J. Bai, J. Billen, J.C. Cai, C. Cheng, L. Du, Q. Du, T.B. Du, W.Q. Guan, X.L. Guan, Y. He, J. Li, J. Stovall, X.W. Wang, J. Wei, Z.F. Xiong, L. Young, H.Y. Zhang, S.X. Zheng, A

3-MeV RFQ accelerator for the Compact Pulsed Hadron Source at Tsinghua University, *Physics Procedia* **26**, 36 (2012).

- [9] C. Zhang, H. Podlech, Efficient focusing, bunching, and acceleration of high current heavy ion beams at low energy, *Nucl. Instrum. Methods Phys. Res., Sect., A* **879**, 19 (2018).
- [10] T.P. Wangler, *RF Linear Accelerators*, (Wiley-VCH Verlag GmbH & Co. KG, 2008).
- [11] I. Hofmann, Emittance Growth of Beams Close to the Space Charge Limit, *IEEE Trans. Nucl. Sci.* **NS-28**, 2399 (1981).
- [12] I. Hofmann, Stability of anisotropic beams with space charge, *Phys. Rev. E* **57**, 4713 (1998).
- [13] R.A. Jameson, in *Proceedings of LINAC1981* (JACoW Santa Fe, USA, 1981), p. 125.
- [14] R.A. Jameson, RFQ designs and beam-loss distributions for IFMIF, Oak Ridge National Laboratory Tech. Rep. ORNL/TM-2007/001, 2007.
- [15] C. Zhang, Z.Y. Guo, A. Schempp, R.A. Jameson, J.E. Chen, and J.X. Fang, Low-beam-loss design of a compact, high-current deuteron radio frequency quadrupole accelerator, *Phys. Rev. ST Accel. Beams* **7**, 100101 (2004).
- [16] W. Simeoni Jr. *et al.*, in *Proceedings of IPAC2011* (JACoW, San Sebastián, Spain, 2011), p. 658.
- [17] TraceWin code, <http://irfu.cea.fr/Sacm/logiciels/>.
- [18] C. Zhang, A. Schempp, Beam dynamics studies on a 200 mA proton radio frequency quadrupole accelerator, *Nucl. Instrum. Methods Phys. Res., Sect., A* **586**, 153 (2008).
- [19] R.H. Stokes *et al.*, in *Proceedings of PAC1979* (JACoW, San Francisco, USA, 1979), p. 3469.
- [20] M. Okamura *et al.*, in *Proceedings of PAC2009* (JACoW, Vancouver, Canada, 2009), p. 4872.
- [21] K.R. Crandall, T.P. Wangler, L.M. Young, J.H. Billen, G.H. Neuschaefer, and D.L. Schrage, RFQ Design Codes, Los Alamos National Laboratory Report No.LA-UR-96-1836, 2005.